



## Laser Application of Nanocomposite Hydrogels on Cancer Cell Viability

Y. Danyuo<sup>1,5,\*</sup>, A. A. Salifu<sup>2</sup>, J. D. Obayemi<sup>2</sup>, C. J. Ani<sup>3</sup>, S. Dozie-Nwachukwu<sup>4</sup>, Theresa Ezenwafor<sup>5</sup>, J. Yirijor<sup>6</sup>

<sup>1</sup> Department of Mechanical Engineering, Ashesi University, Berekuso, Ghana

<sup>2</sup> Department of Mechanical Engineering, Worcester Polytechnic Institute, 100 Institute Road, Worcester, MA 01609, USA.

<sup>3</sup> Department of Theoretical and Applied Physics, African University of Science and Technology (AUST), Km 10, Airport Road, Federal Capital Territory, Abuja Nigeria

<sup>4</sup> Biotechnology Advance Research Center, Sheda Science and Technology Complex (SHESTCO), Abuja, Federal Capital Territory, Nigeria

<sup>5</sup> Department of Materials Science and Engineering, African University of Science and Technology, Federal Capital Territory, Abuja, Nigeria

<sup>6</sup> Academic City College, Department of Mechanical Engineering, Haatso-Accra, Ghana

### Abstract

Nanocomposite hydrogels of poly-*n*-isopropyl were prepared by incorporating gold and magnetite nanoparticles. The nanocomposite-based hydrogels formed were geometrical, ~7.3 mm in diameter and 5 mm thick (in the swollen state). Morphological analysis was characterized by a scanning electron microscope. Drug-loaded hydrogels were subjected to laser heating at 1 W, 1.5 W and 2 W for 20 min in each laser cycle. The metabolic activities of the cells were analysed. The photothermal conversion efficiency of the nanocomposite hydrogels was also evaluated for P(NIPA)-AuNP-PG and P(NIPA)-MNP-PG to be 36.93 and 32.57 %, respectively. The result was then discussed for potential applications whereby metal-based hydrogels can be employed in microfluidic devices for targeted cancer drug delivery.

## 1.0 INTRODUCTION

Breast cancer has contributed majorly to cancer-related mortalities, globally [1,2]. Statistics indicate 1.5 million new cancer cases, with half a million deaths arising, annually [3]. The standard treatment of breast cancer is mainly performed with surgical resections. Other treatment methods include radiotherapy, hormonal therapy, and chemotherapy [4]. These methods are therefore limited due to the higher toxicity of anti-cancer drugs, which also leads to damaging non-target cells.

Thermo-sensitive hydrogels are usually characterized by a lower critical solution temperature (LCST). LCST is a phase transition temperature, which enables the hydrogel to collapse if application temperatures are at or above LCST. This technique is used to induced drug diffusion [5]. In the case of poly-n-isopropyl-acrylamide (P(NIPA))-based hydrogels, significant contributions have been made to study the kinetics of cancer drug release from such gels due to their potential to respond to temperature. The LCST is used to trigger controlled drug release [6-9].

Metal-based nanoparticles have been employed in the treatment of cancer via hyperthermia. The application of magnetite nanoparticles [10] and gold nanoparticles [11,12] have been extensively studied in recent years for their application in cancer treatment. Recent reports show that nanoparticles have higher specificity and hence, could help to curb the negative side effects associated with the conventional cancer treatment methods [13]. In this study, magnetite nanoparticles (MNP) and gold nanoparticles (AuNP) were incorporated into poly-n-isopropyl-acrylamide-based hydrogels. This enables the nanocomposites to generate enough heat through the application of fibre optics laser.

## 2.0 MATERIALS AND METHODS

### 2.1 Materials

Iron oxide nanopowder ( $\text{Fe}_3\text{O}_4$ ) (size range 15-20 nm) with high purity (99.5 %) and AuNP were procured from the US Research Nanomaterials Inc. (Twig Leaf Lane, Houston, USA). N-Isopropylacrylamide (NIPA) with purity 97 % (used as the main monomer), N,N,N',N'-Tetramethyl-ethylene-diamine (TEMED) with purity 99 % was used as a catalyst to accelerate the rate of addition polymerization, N,N'-Methylene-bis-acrylamide (MBA) with purity 99 % was used as a cross-linker, ammonium persulfate (APS) with purity 98 % was used as a radical initiator, and acrylamide (AM) with purity 99.9 % was used as a hydrophilic co-monomer. They were all procured from Sigma Aldrich Company (St. Louis, MO, USA). Human breast cell line (MCF 10A) and human breast carcinoma cell lines, MDA-MB-231 were obtained from the American Type Culture Collection (Manassas, VA, USA).

### 2.2 Polymerization of Nanocomposite-Based Hydrogels

The polymerization of P(NIPA)-based hydrogels was guided by appropriate calculations based on monomers and crosslinkers concentrations as reported earlier [5,8,9].  $\text{Fe}_3\text{O}_4$  nanoparticles were mixed with 10 wt% polyvinylpyrrolidone (PVP) to form a light-viscous solution, while 1 ml of the  $\text{Fe}_3\text{O}_4$ -PVP mixtures were transferred into 7.8 ml of the polymer stock solutions and swirled gently. Similarly, AuNP in

solutions were also added to the polymer solutions. Polymerizations were initiated with 40  $\mu\text{l}$  of TEMED to catalyse the decomposed persulfate ions release [9]. The polymerization process of P(NIPA)- $\text{Fe}_3\text{O}_4$ -based hydrogels as well as P(NIPA)-AuNP-based hydrogels were terminated after 10 s by introducing  $\text{O}_2$  radicals into the solutions. Solid gels were formed within 3 min. The nanocomposite hydrogels were then allowed for 24 h to ensure mechanical strengthening. Subsequently, gels were completely dried at room temperature until constant weights were achieved. Though complete drying tended to collapse the nanocomposite hydrogels, there is a high tendency to recover to natural structure and porosity by expanding, stretching and unfolding coiled chains when incubated in biofluids (pH 7.4) and drug solutions.

### 2.3 Drug Release and Laser Application

The experimental setup for laser application and drug release is shown (Fig.1). During drug delivery, AuNPs-based/MNPs-based hydrogels were loaded with drug solutions, prodigiosin (PDG) for 72 h.

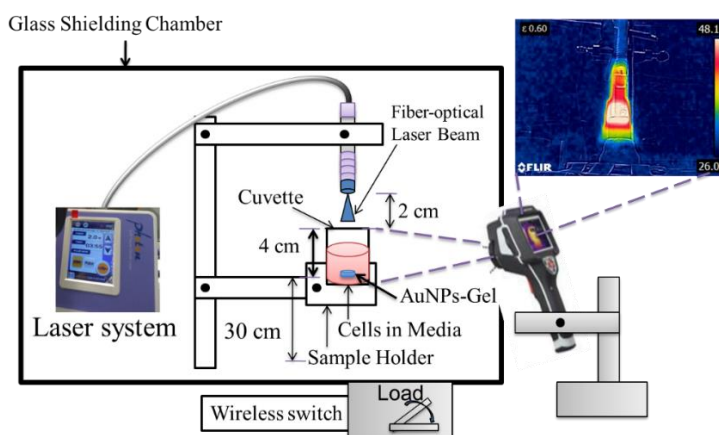


**Figure 1:** Drug Release from AuNP-based Hydrogel and Laser Setup.

The nanocomposite gels were geometrically measured (Mitutoyo Digital Micrometre, Mitutoyo Vernier callipers, Brazil) to be  $\sim 7.3$  mm diameter and 5 mm thick in their swollen state. Drug release was done in a cuvette containing 3 ml phosphate buffer saline (PBS) at pH 7.4. Drug loaded nanocomposite-hydrogels were subjected to laser heating at 1 W, 1.5 W and 2 W for 20 min in each cycle for every 24 h until drug elution were completed. On average, multiples of 30 cycles were conducted for AuNP-based hydrogels, while 35 heating cycles were reported for the MNP-based hydrogels.

### 2.4 Optical and UV-Vis Characterization

P(NIPA)-AuNP/P(NIPA)-MNP composites were coated with gold under vacuum ( $7 \times 10^{-2}$  mBar) using a sputter coater (EMS Quorum, EMS150R ES, Quorum Technologies Ltd, East Sussex, UK). Samples were then mounted on a sample holder, and loaded into Phenom ProX desktop SEM (ThermoFisher Scientific, MA, USA). Morphological differences were observed and reported.

Ultraviolet-visible (UV-Vis) spectrophotometer (Evolution 300, Thermo-Scientific, Shimadzu Scientific Instruments Inc., Marlborough, MA, USA) was used to characterize the absorbance and concentration of the drug released.

## **2.5 FTIR Analysis**

Before sample characterization, the surface of the sample stage was sterilized with acetone to clean up all dirt. FTIR scans were obtained between 500–4000  $\text{cm}^{-1}$  wavenumbers. Functional groups of modified samples were carried out with FTIR analysis (QATR-S, IRSpirit, Thermo scientific, Shimadzu Scientific Instruments Inc., Marlborough, MA, USA). Nanocomposite gels incorporated with gold nanoparticles (AuNPs) as well as magnetite nanoparticles (MNPs) were analysed. Analyses were aided with KnowItAll Chemistry software (Bio-Rad Laboratory Inc., CA, USA). Samples peaks were mapped with identifiable functional groups to ascertain the effect of experimental modifications on the samples.

## **2.6 Drug Release and Laser Application on Cell Viability**

Cell viability via drug release and laser effect was similarly conducted (Fig. 1). MDA-MB-231 and MCF 10A cell lines were used to investigate the effect of drug delivery and laser power on cell viability. Experiments were performed in triplicates. The control samples consist of only cells on culture media on 12 well plates (without any nanocomposite hydrogel) was used for comparison. Experimental samples contained cells cultured on 12 well plates with drug-loaded nanocomposite gels. Samples were incubated at 37°C (CO<sub>2</sub> incubator) set at 5% humidity. Experimental samples containing AuNPs-based/MNPs-based hydrogels were subjected to laser heating at 1 W, 1.5 W and 2 W for 20 min. Three heating cycles were conducted. Thus, after the heating at 0 h (first heating), the experiments were repeated at 24 h, 48 h, and 72 h. Cell viability was accounted using a hemocytometer via an inverted microscope supported with a DS-Qi2 camera (Nikon Eclipse Ts2R, MVI, Avon, MA, USA) according to:

$$\text{Cell Viability} = (V_C/T_C) \times 100 \quad (1)$$

where  $V_C$  is the number of viable cells and  $T_C$  is the total number of cells (include both live and dead cells).

The temperature changes for each laser power were also calculated:

$$\Delta^\circ\text{C} = T_h - T_c \quad (2)$$

where  $T_h$  is the maximum temperature observed and  $T_c$  is the initial temperature.

## **2.7 Fluorescence Staining and metabolic activity**

MCF 10A, MDA-MB-231 cell was fixed with 4% paraformaldehyde for 10 min and then rinsed with DPBS while Triton X100 was used to enhance the permeability of cell membranes. Alexa Fluor 555 Rhodamine Phalloidin (Product # R415, 1:300, Thermo Fisher Scientific, Waltham, MA, USA) was used to stain the actin cytoskeleton for 30 min. SlowFade Gold Antifade Mountant with DAPI (Product # S36938, Thermo Fisher Scientific, Waltham, MA, USA) was used to stain the nuclei of the cells for 10 min. Samples were then placed on glass slides, imaged with Nikon Ts2R-FL inverted fluorescence microscope coupled with a Nikon DS-Fi3 C camera with 20 X and 10 X objectives. (Nikon Instrument Inc., Melville, NY, USA). The fluorometric method (AlamarBlue assay) was then employed, to test the metabolic activity of cells. Fluorescence intensities were determined at 544 nm excitation and 590 nm emission with

the aid of 1420 Victor<sup>3</sup> multi-label plate reader (Perkin Elmer, Waltham, MA). Reduction of Alamar Blue (%) was obtained:

$$\text{Reduction of AlamarBlue (\%)} = \frac{FI_{\text{sample}} - FI_{10\%AB}}{FI_{100\%R} - FI_{10\%AB}} \times 100 \quad (3)$$

where  $FI_{\text{sample}}$  is the experimental fluorescence intensity of samples,  $FI_{10\%AB}$  is the fluorescent intensity of the 10 % Alamar Blue (use as a negative control: an oxidized form of Alamar Blue), and  $FI_{100\%R}$  is the fluorescence intensity of 100 % reduced form of Alamar Blue (use as positive control). Living cells were stained for the nucleus and the cytoskeleton. Cells were similarly fixed with 4 % paraformaldehyde before SEM analysis. Cells were dehydrated with ethanol; 70 %, 80 %, 90 % and 100 % ethanol, respectively at 15 min intervals. Cells were then dried with absolute ethanol-Hexamethyldisilazane (HMDS) at 2:1 ratio, followed by an absolute HMDS. The samples were then dried at absolute ethanol before SEM analysis.

## 2.8 Photothermal Conversion Efficiency

The photothermal conversion efficiency was given by the equation below [14,15]:

$$\eta = \frac{hA(T_h - T_c) - Q_{dis}}{I(1 - 10^{-A_\lambda})} \quad (4)$$

where  $A$  ( $\text{m}^2$ ) is the curvet surface area,  $h$  ( $\text{mW}/\text{m}^2$ ) is the heat transfer coefficient,  $T_h$  ( $^\circ\text{C}$ ) is the maximum temperature in every laser cycle,  $T_c$  ( $^\circ\text{C}$ ) is the room temperature,  $Q_{dis}$  ( $\text{mW}$ ) is the heat dissipated from by the quartz cuvette when filled with cell culture media (L15<sup>+</sup> medium),  $A_\lambda$  is the absorbance of the cell culture media (0.325 at 560 nm wavelength), and  $I$  is referred to as the laser powers (1.0, 1.5 and 2.0 W).

## 3.0 MATERIALS AND METHODS

### 3.1 Morphological Characteristics

Morphologies of the P(NIPA)-based homopolymers are presented in Figure 2(a-c). The SEM images presented consist of P(NIPA) homopolymer as a control sample (with no nanoparticles) (Fig. 2a), P(NIPA)-MNP composite (with 10 wt/wt% MNP) (Fig. 2b), and P(NIPA)-AuNP (with 10 wt/v% AuNP) (Fig. 2c). The scanned micrographs revealed the presence of micropores together with a dispersed nanoparticle. The distribution of MNP and AuNP were spherically dominated in shapes. MNPs were homogenously distributed in the polymer structures. AuNP were accumulated mostly at defects sides and within larger pore regimes. Agglomerated AuNPs were then observed (Fig. 2c). There was a dominance of micro to macropores on the surface of the nanocomposite when AuNP was incorporated. Agglomerated MNPs were also observed as indicated (Fig. 2b) despite several mixings was done (by hand). Due to the high density of the metal nanoparticles, uniform mixing almost becomes a challenge.

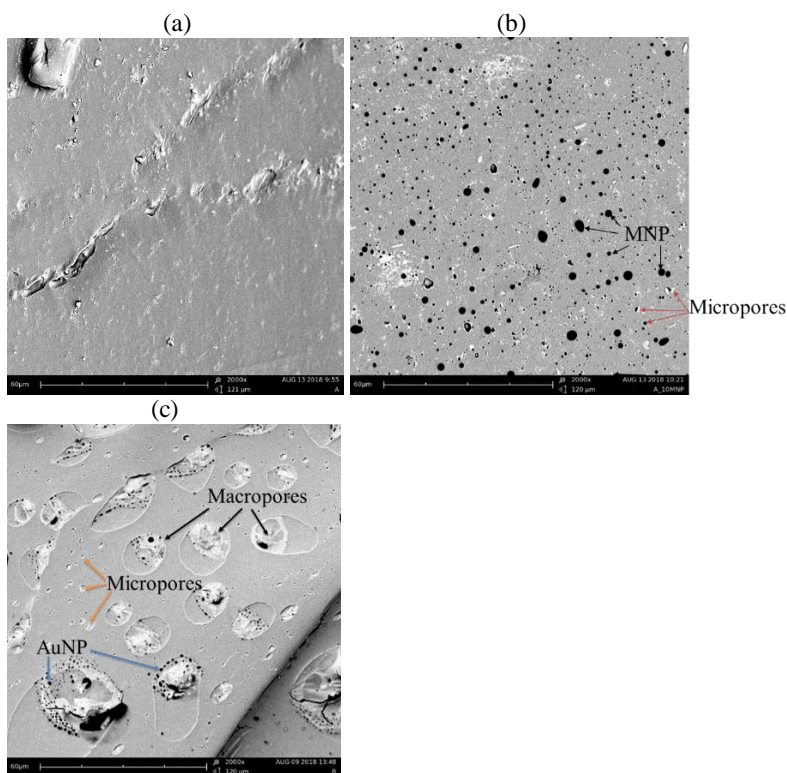


**Figure 2:** Effect of Metal Nanoparticles in P(NIPA)-Based Hydrogels: (a) P(NIPA)-Homopolymer, (b) P(NIPA)- MNP (10 wt/wt% AuNP), and (c) P(NIPA)-AuNP (10 wt/wt % ) with wt% MNPs.

### 3.2 Metabolic Activities of P(NIPA)-Based Hydrogels

MCF 10A cells were stained with Alamar Blue to highlight the metabolic activities of P(NIPA)-based nanocomposites (Fig. 3). The nanocomposite hydrogels used for the metabolic activities were not loaded with any cancer drugs and no laser heating was involved. Though the hydrogels were soaked and washed severally in double distilled water, there could be unreacted salts in the nanocomposite hydrogels which affected the cell-surface interactions and hence, reduced the focal adhesion of the cells to the surfaces. Cells seeded on the nanocomposite hydrogels, therefore, exhibited declined metabolic activities. Though cell metabolism was reduced drastically after day 2, cell population increased gradually on the fourth day (Fig. 3). This indirect measurement of cells-surface coupled with a reduction in metabolic activities, therefore, suggest that P(NIPA) and P(NIPA)-nanocomposite hydrogels should be encapsulated into biocompatible microfluidic devices to enhanced localized chemotherapy [5]. This is clearly outside the scope of the current paper and a challenge for future work.

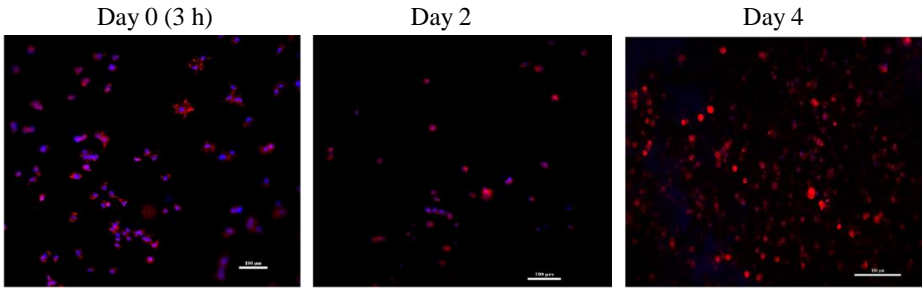


**Figure 3:** Effect of P(NIPA)-MNP on the Metabolic Activities of MCF10A Cell Line. Scale Bars = 100  $\mu\text{m}$ .

### 3.3 Thermal Dose

P(NIPA)-based hydrogels when incorporated with AuNP hydrogels, experienced higher photothermal effects as compared to the magnetite nanocomposite (MNP)-based hydrogels when loaded with prodigiosin (Fig. 4). Similarly, the control sample, P(NIPA)-based hydrogel was also loaded with prodigiosin. This causes a temperature change of 13.9  $^{\circ}\text{C}$  for the AuNP-based hydrogels, while 5.9  $^{\circ}\text{C}$  was the case for MNP-based hydrogels at 1.0 W laser power. The photothermal efficiency for P(NIPA)-Au-PG and P(NIPA)-MNP-PG were 36.93 and 32.57 %, respectively.

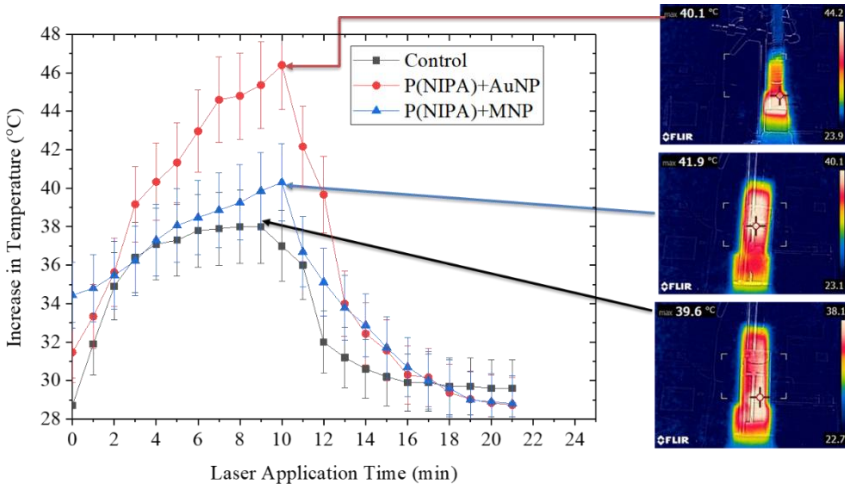


**Figure 4:** Thermal Dose and Temperature Variations at 1.0 W.

### 3.4 Effect of Thermal Dose on Cell Viability

The effect of AuNP on the percentage of cell viabilities is presented in Figure 5a-b. The result (Fig. 5a) indicates an effective decrease in cell population due to varying laser powers from 1.0 W-2.0 W. The metal nanoparticles (eg. gold nanoparticles) hydrogels contributed to local heating within the cell media. This has led to an essential loss of cell viability. Within 72 h, cells subjected to 3 cycle laser heating with gold

nanoparticles-based hydrogels yielded almost 80 % cell death. This means that several heat cycles with this approach can help eliminate localized cancerous cells. Laser ablation such as this could also promote drug diffusion into cancerous tissues (thus laser ablation before drug release).

Percentages of drug release are presented (Fig. 5b). Percentage drug release was found to be prolonged for about 35 days for AuNP-based hydrogels as compared to 28 days for MNP-based hydrogels. Meanwhile, MNP-based hydrogels release a higher dose instantaneously until after 28 days. The photothermal effects of gold and magnetite nanoparticles enable effective drug release.

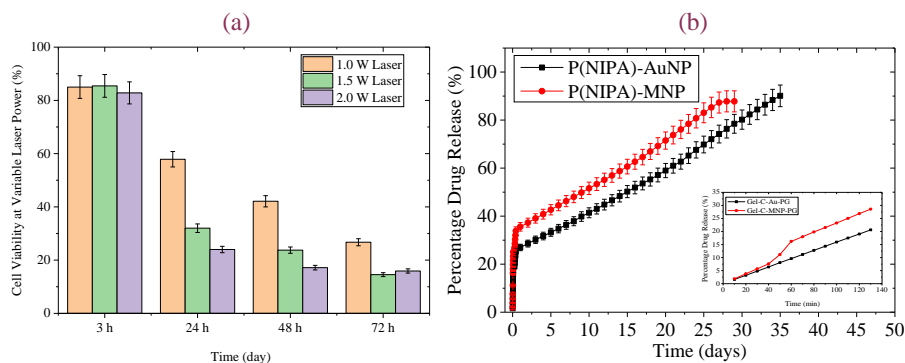


**Figure 5:** (a) Variable Laser Power (20 min) on the Viability of MBA-MD-231 10A Cell Line and (b) Percentage Prodigiosin Drug Release from Metal Nanoparticles. (Error bars are at 5% of data).

## 4.0 CONCLUSION

In this study, magnetite and gold nanoparticles were incorporated into poly-n-isopropyl-acrylamide-based hydrogels to enhance heat induction through the application of a single fiber optics laser beam. Local temperatures were applied at control laser powers (1.0 W, 1.5 W, and 2.0 W). It was observed that 1.5 W could induce enough heat to inhibit cancer cells without affecting normal cells. Recent reports show nanoparticles with higher specificity could help curb the negative side effects associated with conventional cancer treatment methods [13].

It was observed that gold nanocomposite-based hydrogels yielded higher photothermal conditions thereby increasing the matrix and environmental temperatures. This informed us about the unique optical properties of gold and magnetite nanoparticles. AuNP, for example, is known for its surface plasmon resonance effect (SPRE) [16]. The SPRE then results in greater absorption of photons within the visible range.

The metal nanoparticles-based hydrogels contributed to local heating which led to significant loss of cell viability. The cell population was tested by studying the metabolic activities of the cells on the different scaffolds. This indirect measurement of cells-surface adhesion coupled with the reduction in metabolic activities suggests that P(NIPA)-nanocomposite hydrogels should be encapsulated into biocompatible structures to enhanced localized drug delivery as suggested earlier [5]. The results are then discussed for potential methods of incorporating metal-based hydrogels in microfluidic devices for targeted cancer drug delivery. This is clearly outside the scope of the current paper, a challenge for the future.

## Acknowledgments

The authors appreciate the support of the Pan-African Materials Institute (PAMI) (Grant No. P126974) for funding this project. We also appreciate the Ashesi University, Ghana and the Worcester Polytechnic Institute (WPI) USA for providing the enabling resources for the execution of this project.

## References

- [1] Levaggi, A., Poggio, F., and Lambertini, M. (2014). The burden of breast cancer from China to Italy. *Journal of Thoracic Disease*, 6(6), 591-594.
- [2] Zhang, W., Becciolini, A., Biggeri, A., Pacini, P., and Muirhead, C. R. Second malignancies in breast cancer patients following radiotherapy: a study in Florence, Italy. *Breast Cancer Research*. (2011).
- [3] Shachar, S. S. and Muss, H. B. Assessing Treatment Response in Metastatic Breast Cancer. *American Journal of Hematology/Oncology*, 12(6) (2016) 6-10.
- [4] Madani, S. Y., Naderi, N., Dissanayake, O., Tan, A., & Seifalian, A. M. (2011). A new era of cancer treatment: Carbon nanotubes as drug delivery tools. *International Journal of Nanomedicine*, 6 (2011) (2963-2979).
- [5] Danyuo, Y., Obayemi, J. D., Dozie-nwachukwu, S., Ani, C. J., Odusanya, O. S., Oni, Y., and Anuku, N. Prodigiosin release from an implantable biomedical device: kinetics of localized cancer drug release. *Mater. Sci. and Engr. C*, 42 (2014) 734-745.
- [6] Oni, Y., Theriault, C., Hoek, A. V. and Soboyejo, W. O. Effects of Temperature on Diffusion from PNIPA-Based Gels in a BioMEMS Device for Localized Chemotherapy and Hyperthermia. *Mater. Sci. Eng. C* 31(2011) 67-76.
- [7] Zhang, J., Cheng, S., Huang, S. and Zhuo, R. Temperature-Sensitive Poly (N - isopropylacrylamide) Hydrogels with Macroporous Structure and Fast Response Rate. *Macromol. Rapid Commun.* 24 (2003) 447-451.
- [8] Danyuo Y., Dozie-Nwachukwu S., Obayemi J. D., Ani C. J., Odusanya O. S., Oni Y., Anuku N., Malatesta K. and Soboyejo W. O. Swelling of Poly (N-isopropyl acrylamide) (PNIPA)-Based Hydrogels with Bacterial-Synthesized Prodigiosin for Localized Cancer Drug Delivery. *Mater. Sci. and Engr. C (MSEC)* 59 (2016) 19-29.
- [9] Danyuo Y., Ani C. J., Salifu A. A., Obayemi J. D., Dozie-Nwachukwu S., Obanawu V. O., Akpan U. M., Odusanya O. S., Abade-Abugre M., McBagonluri F. and Soboyejo W. O. Anomalous Release Kinetics of Prodigiosin from Poly-N-Isopropyl-Acrylamid based Hydrogels for The Treatment of Triple Negative Breast Cancer. *Scientific Reports*. 9 (2019) 3862.
- [10] Obayemi J. D., Dozie-Nwachukwu S., Danyuo Y., Odusanya O. S., Anuku N., Malatesta K. and Soboyejo W. O. Biosynthesis and the Conjugation of Magnetite Nanoparticles with Luteinizing Hormone Releasing Hormone (LHRH). *ELSEVIER; Materials Science and Engineering C (MSEC)*. 46 (2015) 482-496.
- [11] Dozie-Nwachukwu S. O., Obayemi J. D., Danyuo Y., Etuk-Udo G., Anuku N., Odusanya O.S., Malatesta K., Chi C. and Soboyejo W.O. *Advanced Materials for Sustainable Development*. Editors: W. Soboyejo, S. Odusanya, Z. Kana, N. Anukwu, K. Malatesta and M. Dauda. Biosynthesis of Gold Nanoparticles with *Serratia marcescens* Bacteria. *Trans Tech Publications, Switzerland. Book of proceedings*. 1132 (2016) 51-71.
- [12] Dozie-Nwachukwu S., Obayemi J. D., Danyuo Y., Jingjie H., Cathy C., Anuku N., Odusanya O. S., Malatesta K. and Soboyejo W. O. A Comparative Study of the Adhesion of Biosynthesized Gold and Conjugated Gold/Prodigiosin Nanoparticles to Triple Negative Breast Cancer Cells. *J. of Mater. Sci.: Mater. in Med. (JMSM)*, 28 (2017) 143.
- [13] Xiaoming L., Guangshuai S., Junsheng Y., Wei Y., Zhaodi R., Xiaohui W., Xi X., Hui-Juan C. and Xiaodong C. Laser heating of metallic nanoparticles for photothermal ablation applications. *AIP Advances*. 7, (2017) 025308.
- [14] Xijian L., Bo L., Fanfan F., Kaibing X., Rujia Z., Qian W., Bingjie Z., Zhigang C. and Junqing H. Facile synthesis of biocompatible cysteine-coated cus nanoparticles with high photothermal conversion efficiency for cancer therapy. *The Royal Society of Chemistry Dalton Transactions*. 30, (2014).
- [15] Hessel C. M., Pattani V. P., Rasch M., Panthani M. G., Koo B., Tunnell J. W. and Korgel B. Copper Selenide Nanocrystals for Photothermal Therapy. *A., Nano Lett.* 11 (2011) 2560-2566.
- [16] Xiaohua Huang, Mostafa A. El-Sayed. Gold nanoparticles: Optical properties and implementations in cancer diagnosis and photothermal therapy. *J Adv Res.* 1(1) (2010)13-28.